Moroccan Journal of Chemistry
ISSN : 2351-812X

Mor. J. Chem., 2023, Volume 11, Issue 01, Page 265-281
https://revues.imist.ma/index.php/morjchem

Kinetic, isotherm and thermodynamic studies on the adsorption of Methylene blue dye using Moringa oleifera pods and kernels

Fadimatou Ahmadou[1], Fatima-Zahra Abahdou[1], Rachid Slimani[1] and Souad El Hajjaji[1,*]

[1]*Laboratory of spectroscopy, Molecular Modeling, Materials, Nanomaterials, Water and Environment, (LS3MN2E-CERNE2D), Faculty of Sciences, Mohammed V University in Rabat, Morocco.*
**Corresponding author, Email address: s.elhajjaji@um5r.ac.ma*

Received *25 Oct 2022,*
Revised *24 Jan 2023,*
Accepted *27 Jan 2023*

Citation*: Ahmadou F., Abahdou F. Z., Slimani R. El Hajjaji S. (2023) Kinetic, isotherm and thermodynamic studies on the adsorption of Methylene blue dye using Moringa oleifera pods and kernels, Mor. J. Chem., 14(1), 265-281. Doi: https://doi.org/10.48317/IMIST.PRSM/morjchem-v11i1.34864*

Abstract: The low availability of water resources and the difficulty of access to drinking water are of increasing concern. To face this problem, it is important to improve the quality and quantity of this resource by fighting mainly against its pollution. Thus, it has become necessary to treat the wastewater of industries. In this work we studied the adsorption of methylene blue onto waste of the Moringa oleifera seeds with the aim of valorizing the natural biomass. To understand the adsorption process of Moringa oleifera pods powder and Moringa oleifera kernels powder various studies were performed. Most characterizations of adsorbent like Fourier transform infrared spectroscopy (FT-IR), X-ray diffraction (XRD), scanning electronic microscopy (SEM), specific surface by BET and pHpzc were investigated. The effects of parts of adsorbent, pH of solution, adsorbent dose, initial dye concentration, temperature and contact time on the batch adsorption of methylene blue on Moringa oleifera pods powder (MOPP) and Moringa oleifera kernels powder were studied. The Kinetic, isotherms and thermodynamic studies were done. The adsorption results of methylene blue onto Moringa oleifera pods powder and Moringa oleifera kernels powder showed that the pseudo-second order is the best model with a good correlation. The adsorption isotherm data for the two adsorbents was best correlated with Freundlich isotherm. The values of thermodynamic parameters show that adsorption is an exothermic process for MOPP and MOKP. However, the negative value of the ΔG° indicated that the adsorption of methylene bleu on adsorbents was thermodynamically feasible and spontaneous.

Keywords: Adsorption, methylene blue, Moringa oleifera, kinetics study, isotherm models, thermodynamic study.

1. Introduction

Environmental and water pollution is a major problem in developing countries. But water pollution remains more worrying for humans, hence the involvement of national and international organizations. It is caused by the presence of certain contaminants such as dyes. Dyes are used in several sectors such as cosmetics, printing, food, pharmaceutical and especially textile industries. The global production of dyes is estimated at more than 800,000 tons per year (Mansour *et al.,* 2011). The discharge of these contaminated waters into receiving surface waters causes water pollution on Earth

and greatly affects the health of all life forms (Çelekli *et al.,* 2019). Treatment of these waters before discharge becomes necessary (Bouknana *et al.,* 2014).

Several approaches have been utilized for removing dyes from the wastewater such as coagulation-flocculation, membrane filtration, chemical oxidation, photocatalytic degradation, electrochemical degradation, sonocatalytic degradation, ion exchange, reverse osmosis, electrochemical methods, and adsorption (Shirani *et al.,* 2018; Karoui *et al.,* 2020). Some of these technics have some disadvantages. However, adsorption technic is approved as a simple and efficient technique for the removal of undesired compounds using low-cost various materials (Singh *et al.,* 2017).

In recent years, emphasis has been placed to use sustainable ways to clean up wastewater and specially to protect the environment. To this end, researchers have focused on the use of biomaterials from various organisms and agricultural by-products for the treatment of wastewater containing undesirable compounds such as dyes, metals, etc. Biomaterials offer many benefits such as easily accessible, show good adsorption capacity for a variety of pollutants (even at low concentrations), do not require any processing, being environmentally friendly and locally available at very low cost (Cardoso *et al.,* 2017) and finally have the potential to be conveniently regenerated (Maina *et al.,* 2016).

For our study, agricultural materials such as Moringa oleifera waste seeds will be used in the treatment of waste, it has shown its efficiency as coagulants (Camacho *et al.,* 2017; Reck *et al.,*2018) and bio adsorbents in the removal of toxic compounds like dye (Çelekli *et al.,* 2019; Soliman *et al.,* 2019; Oba & Adekola, 2018), toxic aquatic pollutants (Shirani *et al.,* 2018) etc, replacing synthetic chemicals. The choice of Moringa oleifera for this study lies in the fact that it is available in large quantities and is relatively inexpensive.

This paper evaluates the capacity of different Moringa oleifera (MO) for the adsorption of methylene blue (MB). To achieve this, some analyses of the wastes have been done, like FTIR, DRX, SEM, BET and pH_{pzc}. In addition, several studies were carried out: the kinetic study, the isotherm and the thermodynamics in order to understand the adsorption process. The results of the equilibrium study has been be treated according to the mathematical models of Langmuir, Freundlich and Temkin isotherms to determine the maximum adsorption capacity and the influencing parameters of adsorption.

2. Material and methods

2.1. Adsorbents

Moringa oleifera seeds were collected in the family garden located in Maroua in the Far North region of Cameroon. These seeds were air-dried for a week. Cleaned and suitable seeds were selected for experiments.

2.1.1. Moringa oleifera pods powder

Moringa oleifera seeds were shelled manually to remove the pods. The pods were washed with deionized water to remove any impurity from the pods and dried in an oven at 45° C overnight. The washed pods were then ground with the grinder and the obtained *Moringa oleifera* pods powder (MOPP) was washed and dried in the oven for 24h. That is the MOPP which was used for experiments.

2.1.2. Moringa oleifera kernels powder

The grains, obtained after husking, were washed with distilled water and dried in an oven at 45 °C for 6 hours and left overnight in the open air. They were then ground using a brand electric grinder until a powder was obtained. This powder was used for the extraction of MO oil by the Soxhlet method. The residue obtained after extraction of the oil was dried at room temperature in the open air for 24 hours

and then collected and dried again for 24 hours at 60 °C. It was this final residue that we called *Moringa oleifera* kernels powder (MOKP) that we used for the adsorption experiments.

2.2. Adsorbat

Methylene Blue had been used and his formula is $C_{16}H_{18}N_3S$. His λ_{max} is 664 nm. The cationic dye MB is used without further purification.

2.3. Methods

2.3.1. Characterizations of the different Moringa oleifera wastes

The *different Moringa oleifera wastes* was characterized using FT-IR and XRD analysis. The FT-IR spectra were obtained using IRTF Vertex 70. While the XRD of *Moringa oleifera wastes* biosorbent was carried out by using PANalytical's X'Pert PRO MRD using copper anode tube λ(Cu) = 1.54 Aº. The micrographs of sample were taken using scanning electron microscopy (SEM) (FEI Quanta 200) and the surface areas were calculated by the BET (Brunaauer-Emmett-Teller) method.

2.3.2. Determination of point zero charge

The pH_{pzc} called zero charge point pH, corresponds to the pH value for which the material surface charge is zero. To determine the pH_{pzc} of our adsorbent, 50 mL of 0.01 M sodium chloride (NaCl) solution was taken and placed in 7 beakers then the pH was adjusted between 2 and 12 by adding a few drops of NaOH or HCl solution (0.1 M). Then 0.1 g of the adsorbent was added to each beaker. The suspensions were stirred at room temperature for 24 h. the final pH values pH_f were measured. The pH_{zpc} which is the point of intersection corresponding to the plot of the curve f (pH) = (pH_f - pH_i) was determined by simple reading (Utrilla *et al*., 2001, Bencheikh *et al.,* 2021).

2.3.3. Adsorption experiments

For carrying out the adsorption tests, several values of pH, mass of the adsorbent and concentration of the adsorbent were considered. All conditions met, the solution of 50 ml of the adsorbent - adsorbate mixture was stirred for 90 min. The colored solution obtained at the end of the experiment was separated from the adsorbent by centrifugation with Sigma 2-15 Centrifuge at a speed of 3000 rpm for 15 min. The absorbance of the supernatant was measured using a UV / visible spectrophotometer of the MAPADA V-1200 type at the wavelength 660 nm which is that of methylene blue (MB). The adsorption capacity of the dye by different MO wastes was calculated using the following formula:

$$\boldsymbol{Q_t = \frac{C_O - C_t}{m}.V} \qquad \textbf{(eq.1)}$$

Where:

Q_t (mg. g^{-1}) is the amount adsorbed at time t (min);

C_0 (mg / L) is the initial dye concentration.

C_t (mg / L) is the dye concentration at time t;

V is the volume of the solution (L) and

m is the amount of the adsorbent in solution (g).

And the removal efficiency of dye which is determined by the following equation:

$$\boldsymbol{R(\%) = \frac{C_O - C_{eq}}{C_{eq}} \times 100} \qquad \textbf{(eq. 2)}$$

With C_0: Initial concentration in mg/L and C_e: Equilibrium concentration in mg/L.

3. Results and discussion

3.1. Characterization of Moringa oleifera pods and kernels powders

3.1.1. Fourier transform infrared spectroscopy (FT-IR) analysis

The FTIR spectroscopic analysis of the pods and kernels of *Moringa oleifera* is shown in **Figure 1** and **Figure 2** respectively. The Fourier Transform Infrared Spectroscopy (FTIR) spectra for moringa seeds show the presence of hydroxyl groups, proteins, fatty acids, carbohydrates and lignin (Baptista *et al.,* 2017; Alves *et al.,* 2010). Thus, in general, the FTIR's spectra of moringa seeds showed the presence of various functional groups, indicating their complex nature which indicated broad band at 3292.97 cm^{-1} representing the functional group -OH stretching, his functional group appears predominantly in the protein and fatty acid structures present in Moringa seeds (pods) (Araujo *et al.,* 2018, Alsharaa et *al.,* 2016).

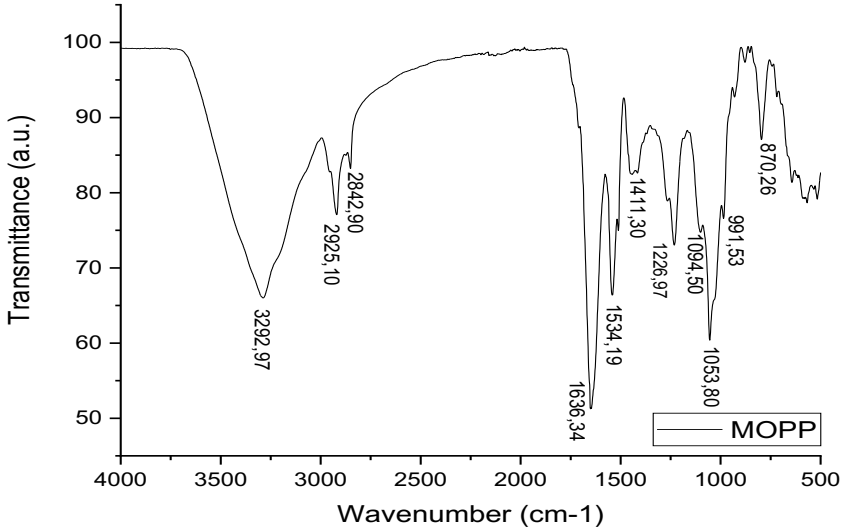

Fig. 1: FTIR spectrum of *Moringa oleifera* pods powder (MOPP).

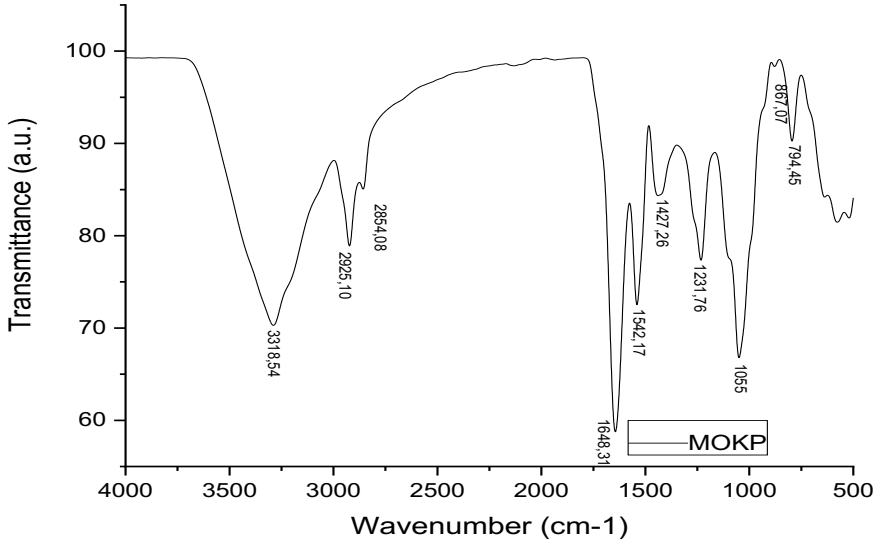

Fig. 2: FTIR spectrum of *Moringa oleifera* kernels powders (MOPK).

The band at 2925.10 cm^{-1}corresponds to the symmetrical and asymmetrical stretching of C-H of CHO. There is also a band at 1636.34 cm^{-1} and 1534.19 cm^{-1} which correspond to the water absorbed by the cellulose (Olsson and Salmen, 2004). The band around 1411.30 cm^{-1} is associated with the symmetrical CH_2 deformations present in cellulose (Paiva *et al*., 2007) while the band 1226.97cm^{-1} in the spectrum is attributed to the valence vibrations of the CH and C=O groups of the aromatic polysaccharide ring (Sgriccia *et al.,* 2008). The absorption band at 1094.50 cm^{-1} corresponds to the vibration of the C=O band of the acetyl group present in lignin and hemicellulose. The peak at 1053.80 cm^{-1} is attributed to the valence vibrations of the –C-O and O-H groups in cellulose (Arrakhiz *et al.,* 2013). The major functional groups found in the kernels were characterized by FTIR. The broad band centered at 3318.51cm^{-1} can be attributed to O-H stretching of the bond in the protein, fatty acid, carbohydrate and lignin units. Since the protein content of the seed is high, this region also shows a significant contribution due to N-H stretching of the amide bond (Araújo *et al.,* 2010).

The two bands observed at 2925.10 and 2852.08 cm^{-1} represent the asymmetric and symmetric stretching of the C-H bond in the CH_2 (Ezeamaku *et al.,* 2018). The high intensity of these two bands could be attributed to the lipid component of the seed, which is present in high amounts, just like the protein. The band at 1648.31 cm^{-1} shows the C=O stretching of the amide carbonyl group in the protein moiety (Araújo *et al.,* 2010). The band at 1542.17 cm^{-1} corresponds to the C=C stretching of alkenes in the aromatic ring with medium and multiple bands, while the peak at 1427.26 cm^{-1} shows the -C-H deformation of the alkane group while 1231.76 cm^{-1} represents the C-N stretching of the amine group and the deformation of the N-H bonding proteins present in the seed (Ravikumar and Udayakumar, 2020). The band at 1055.7 cm^{-1} indicates the coupling mode of C-O stretching and ester stretching vibrations with two or more bands.

3.1.2. X- ray diffraction (XRD) analysis

The X-ray diffraction spectra of the pods and kernels powders of *Moringa oleifera* are shown in **Figure 3** and **Figure 4** respectively. The **Figure 3** shows that the pod, presented peaks at different angles; the first, 2θ = 37°, and the second, 2θ = 44°, indicate the presence of graphite structure, in turn, represents a regularity in the crystalline structure correspond to the high content of cellulose, which results in a better alignment of the layers (Reck *et al.,* 2018).

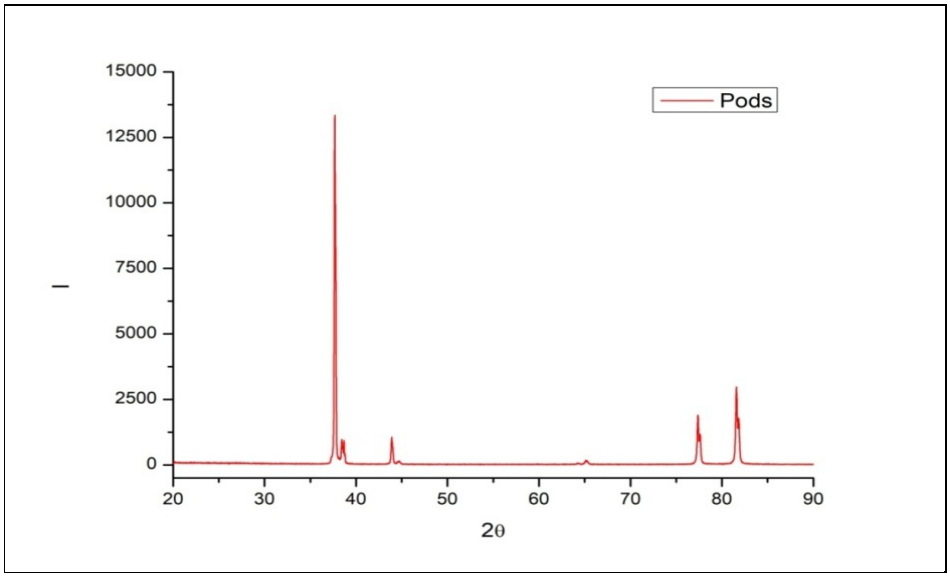

Fig. 3: X-ray diffraction spectrum of the *Moringa oleifera* pods powder (MOPP).

However the noticeable hump for the **figure 4** in the 2 theta range, 20°–30°, signifies a high degree of disorder, probably due to the high amount of oils and proteins content in *Moringa* seeds (kernels) (Araujo *et al.,* 2010, Reck *et al*., 2018). The peaks at 37.2° and 44.3° signifying the presence of graphite structure in *Moringa* pods and kernels respectively.

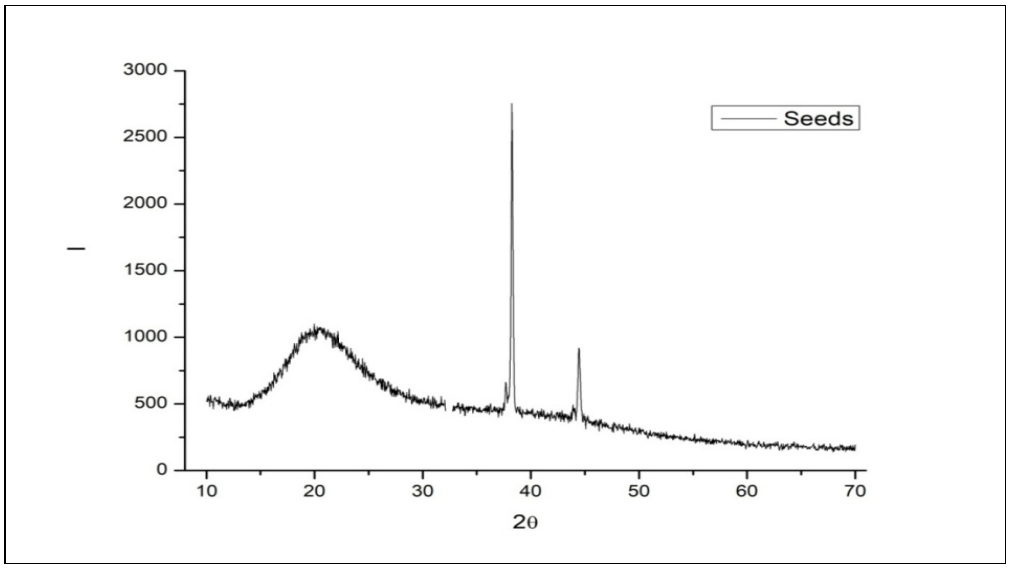

Fig. 4: X-ray diffraction spectrum of the *Moringa oleifera* kernels powder (MOKP).

3.1.3. Scanning electron microscopy (SEM) of different waste biosorbent

The surface morphology of the biosorbent observed by SEM depicted in **Figure 5a** and **Figure 5b** indicates a heterogeneous and porous morphology with tiny particles of various sizes for the pods and kernels of *Moringa oleifera* (Alsharaa *et al.,* 2016). The spaces available facilitate the adsorption process because they provide a high internal surface area. Thus, based on these characteristics, it can be concluded that these materials have an adequate morphological profile for retaining dyes likes MB.

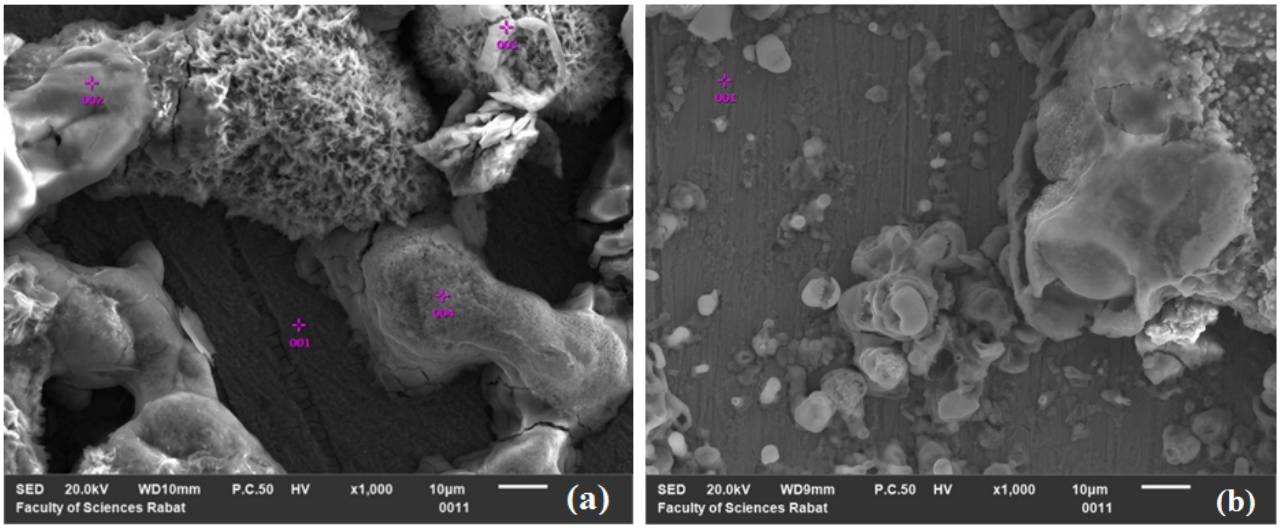

Fig. 5: The SEM micrographs of different wastes of MO: (a) kernels seeds, (b) pods

3.1.4. Surface areas of different waste biosorbent

The surface areas of the kernels and the pods of *Moringa oleifera* determined by BET method were found 1000 and 2000 cm^2/g, respectively, for kernels and pods.

3.1.5. Determination of zero-point charge

The determination of the pH_{pzc} value of the tested materials show the surface charge of these different materials. Generally, the cationic adsorbate tends to adsorb on the adsorbent at pH > pH_{pzc} then that the net surface charge of the biomass is negative, while the adsorption occurs for the anionic adsorbate at pH < pH_{pzc} then that the net surface charge of the biomass is positive (Filho *et al.,* 2017; Azoulay *et al.,* 2020). The pH_{pzc} of kernels and pods was found respectively to be 7.31 and 6.94 (**figure 6a** and **figure 6b**). These results showed that the kernels and pods had varying electrostatic charges under different pH conditions. In an alkaline medium, the material was negatively charged; however, the charge turned positive when the material was studied in an acid medium. These characteristics of the grains and pods suggest that they can interact favorably with a positively charged adsorbate in basic medium and this is in good agreement with the results obtained by the pH effect. For this reason, the maximum sorption efficiency may be due to the interaction between MB and the surface of the two adsorbents.

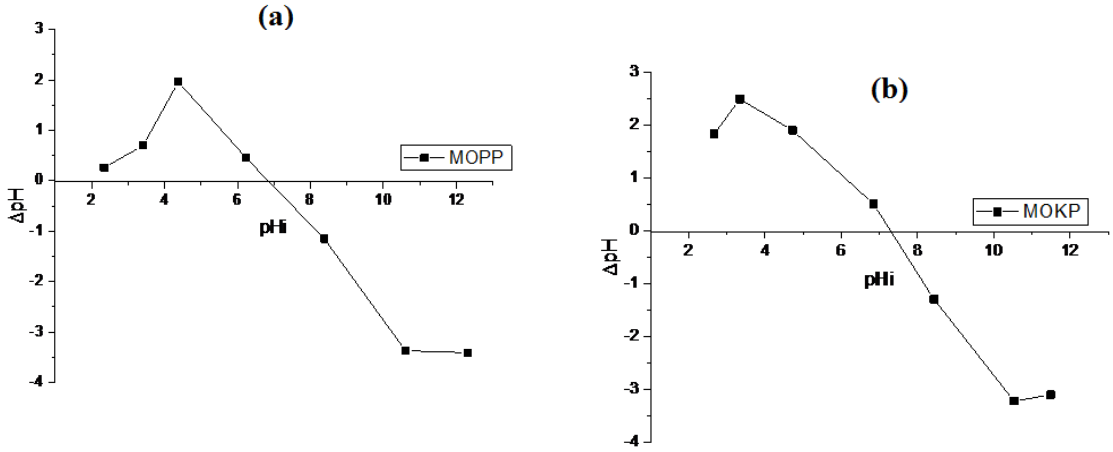

Fig. 6: The pH_{pzc} of different wastes of MO: (a) kernels seeds, (b) pods

3.2. Effects of certain parameters in the adsorption phenomenon

3.2.1. Effect of adsorbent dosage

Adsorbent dosage is a mainly important parameter to determine the capacity of an adsorbent removal the adsorbate as well as the economics of process. To study the effect of adsorbent dosage on Methylene Blue adsorption, different amounts of pods and kernels powder of *Moringa oleifera* from 0.5 to 3 g/L were used at ambient temperature and contact time of 60 min for fixed initial Methylene Blue concentration of 20 mg/L without pH adjustment. The results obtained are shown in **Figure 7**. From **figure 7**, it observed that the adsorption capacity of MB increases with an increase of adsorbent dosage. The removal of MB increased from 96.40 to 99.32% for the pods powder of Moringa oleifera and from 41.55 to 72.12% for the kernels powder of Moringa by increasing the amount dose from 0.5 to 3 g/ L. This increase could be attributed to increases in the adsorbent surface areas, increasing the number of adsorption sites available for adsorption (Hu *et al.,* 2010; Soliman *et al.,* 2019).

3.2.2. Effect of Initial Concentration of Adsorbate

The adsorption of methylene blue was studied by taking the following constants: 0.5 g/L for pods and 1 g/L for kernels as dose, 60 minutes of contact time, a temperature of 25°C, and different concentrations of adsorbate (10 mg/L to 50 mg/L). The effect of initial dye concentration on the pods and Kernels powder of Moringa oleifera adsorption is shown in **Figure 8**. As can be seen from **Figure**

8, the adsorption capacity increased as the initial dye concentration increased, it achieved 88.51 mg/g and 81.68 mg/g for the pods and the seeds of MO successively, at an initial concentration of 60 mg/L. The effect of initial concentration of adsorbate on the capacity of MB removal can be explained in terms of the number of available free surfaces sites in adsorbent structure and adsorbate / adsorbent ratios. The remaining sites had greater resistance to being occupied due to the repulsive forces between the dye adsorbed onto the biomass Moringa kernels and pods solution (Reck *et al.,* 2018).

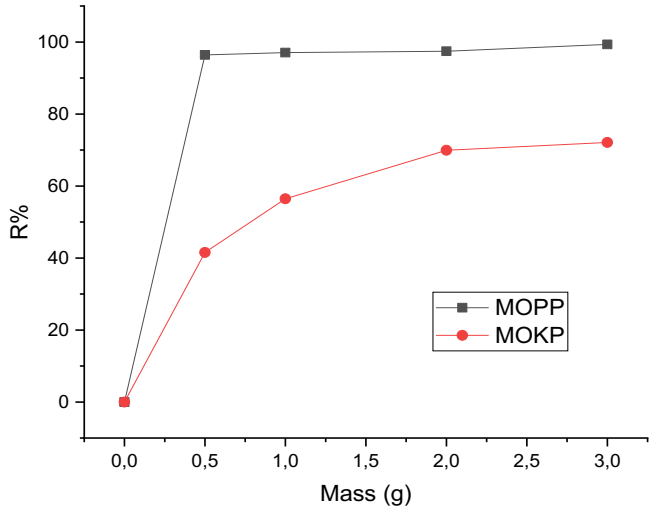

Fig. 7: Effect of adsorbent dose on the adsorption of Methylene Blue by the pods and kernels powder of *Moringa oleifera*. Concentration = 20 mg/L; Time = 60 min; Temperature = 25 °C.

At higher initial concentrations, the active sites of prepared adsorbent would be surrounded with more MB molecules in the solution; hence the equilibrium adsorption capacity of pods and kernels wastes increases with increasing the MB molecules concentration which favorize the adsorption process (Kali *et al.,* 2022). These results are similar with their Soliman *et al.,* 2019 who were found a rapid and higher adsorption of Congo red and Dispersed red 60 dyes with *Moringa oleifera* seeds waste as adsorbent observed during the initial stage then it slowed down till it reached the equilibrium state.

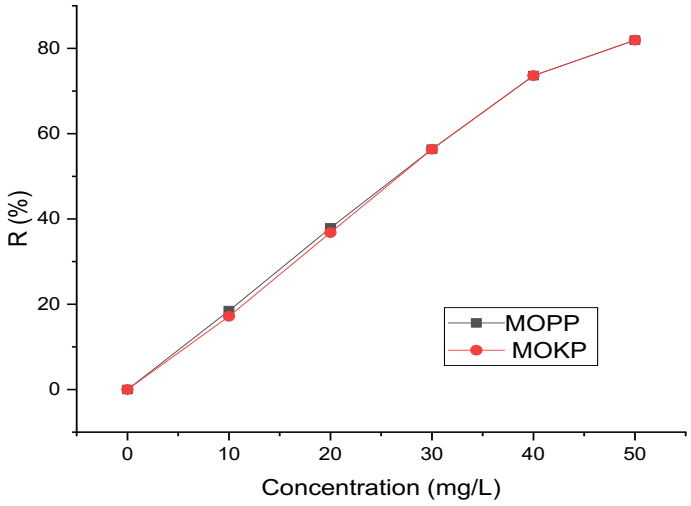

Fig.8: Effect of initial dye concentration on the adsorption of MB onto MOPP and MOKP kernels. Mass of pods = 0.5 g/L; Mass of kernels = 1g; Time = 60 min; Tp = 25 °C

3.2.3. Effect of pH

The influence of the initial pH of the solutions on the adsorption was studied in the range of 3 to 11. The influence of the initial pH of the dye solution on the adsorption of MB onto the pods and kernels powder of Moringa oleifera is presented in **Figure 9**. The influence of the initial pH of the solutions on the adsorption was studied in the range 3 to 11. The amounts of dye retained by the adsorbent from different solutions were found to be closely related to the initial pH value of the solution as moved in **Figure 9**. The retention rates are appreciable between 4 and 11 for pods with a significant retention peak around pH=5 thereafter noticing a slight decrease from ~92% to ~88% at pH=7 and above pH=7, the retention of MB decreases. Contrary to the pods the kernels its retention rate is appreciable between the pH values between 4 and 9, with an important peak of retention towards pH=9, then a slight decrease of efficiency is observed with the increase of the pH, until pH11 the rate decreases from ~ 96 to ~ 90 % between these two values.

It can be seen from the **figure 9**, that the adsorption of MB increased with the increase of initial solution pH. To explain this increase, we need to use the value of the pH_{pzc} shown in the **figure 6.** At values of pH < pH_{pzc}, the surface charges of the tested adsorbents are positive and available to bind cationic dye such as MB. At pH > pH_{pzc}, the adsorbent surface is negatively charged and susceptible to electrostatic interactions with anionic dye molecule as MB. Also, the change of pH affects the adsorptive process through dissociation of functional groups on the adsorbent surface active sites (Aysan *et al.*, 2016; El Hammari *et al.*, 2022). Additionally, lower sorption of MB at acidic pH is due to the presence of excess H^+ ions competing with dye cations for the adsorption sites of powder prepared from the pods and kernels of *Moringa oleifera* (Djelloul *et al.,* 2017).

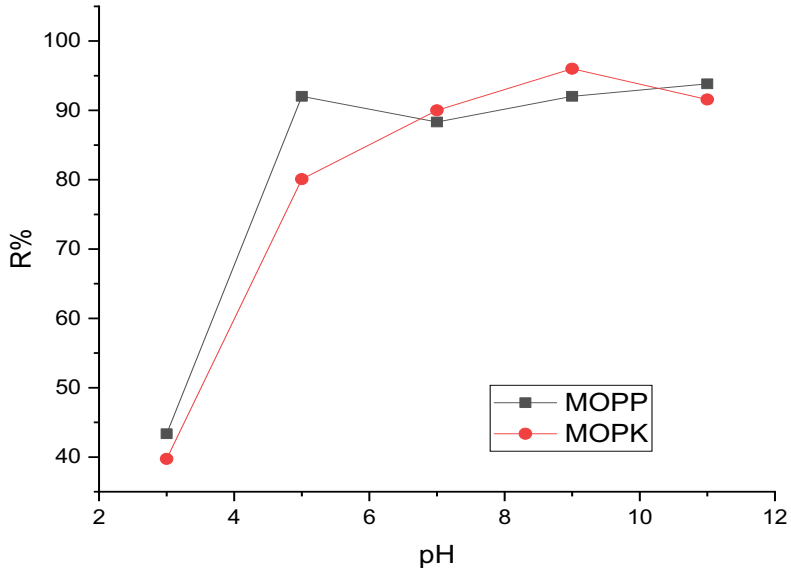

Fig. 9: Effect of pH on the adsorption of Methylene Blue by the MOPPand the MOPK. Mass of pods = 0.5 g/L and mass of kernels = 1g/L; Time = 60 min; Tp = 25 °C; Conc = 20 mg/L.

3.2.4. Effect of the temperature

To study of the parameters affecting the adsorption process we must take into account to the effect of the temperature of the solution. Three different temperatures were tested. According to **Figure 10**, it can be seen that with the increasing temperature from 25°C to 45°C decreased the adsorption capacity

from 90.86 to 85.97 mg/g and from 89.64 to 83.18 mg/g onto the pods and the kernels powder of *Moringa oleifera* successively, This suggests that the effect of temperature is an exothermic nature on the adsorption process. An increase of temperature increases the rate of diffusion of the adsorbate molecules across the external boundary layer and within the internal pores of the adsorbent particle, due to the decrease in the viscosity of the solution (Ghasemi et al., 2007, Djelloul et al., 2017).

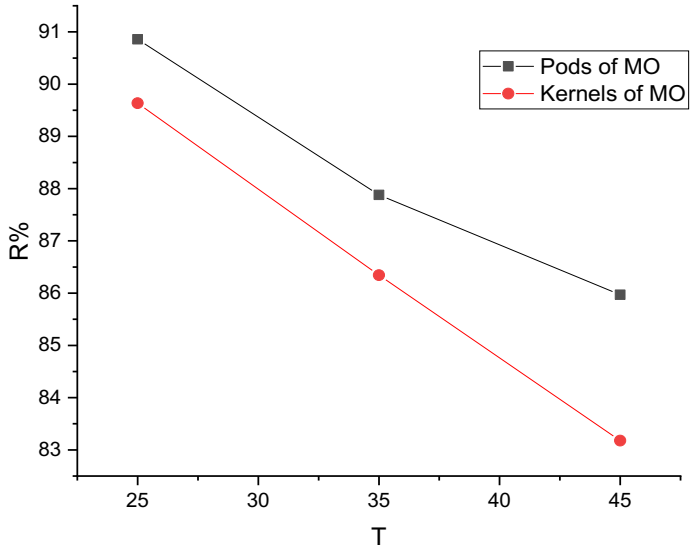

Fig. 10: Effect of temperature on the adsorption of Methylene Blue by the pods (MOPP) and the kernels (MOKP) of *Moringa oleifera*.

3.2.4. Effect of the contact time

The contact time is an influential parameter in the adsorption studies. Different masses are used to evaluate the adsorption kinetics on pods and kernels. **Figures 11** show that adsorption occurs rapidly in the first 10 minutes of contact followed by a slow increase until reaching the equilibrium around 30 min state for the different adsorbents. The fast uptake in the first stage was attributed to abundant unoccupied active functional sites were easily accessible (Shooto *et al.*, 2020). The evolution observed in the second part can be explained by saturation of the specific surface of the adsorbent.

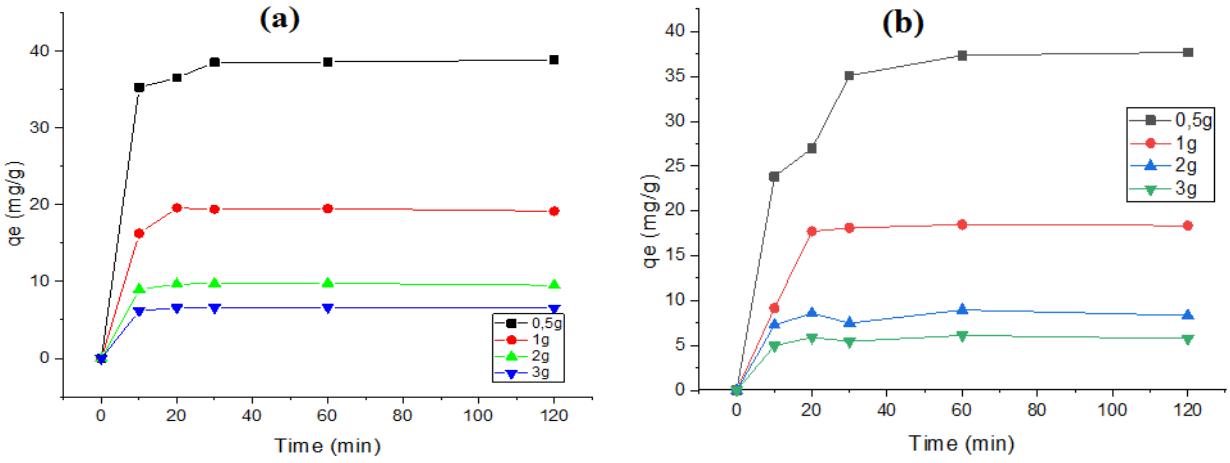

Fig. 11: Effect of contact time on the adsorption of Methylene Blue by the pods (MOPP) and the kernels (MOKP) of *Moringa oleifera*. Mass of pods = 0.5 g/L and mass of kernels = 1g/L; Tp = 25°C; Conc=20 mg/L

3.3. Adsorption kinetics

Kinetics of adsorption is one of the important characteristics to better understand the mechanism of adsorption. Tow kinetic models are applied in the present study, the pseudo-first-order and the pseudo-second-order model in order to investigate the mechanism of the adsorption of MB on the pods and the kernels of *Moringa oleifera*. The biosorption data were analyzed according to the pseudo first-order kinetic model. Values of the rate constant (k_1), equilibrium biosorption capacity ($q_{e,cal}$), and correlation coefficient (R^2) were calculated from the plots of ln(qe qt) versus t (figure not shown) and are presented in Table 1. Kinetic data were further treated with the pseudo-second-order kinetic model. Values of the rate constant (k_2), equilibrium biosorption capacity ($q_{e,cal}$), the correlation coefficient (R^2) were calculated from the slope and intercept of the plots of t/qt against t as shown in Figure 12 and are presented in Table 1.

Table 1. The pseudo first-order and second-order adsorption rate constants and experimental qe values for the pods and the kernels of *Moringa oleifera*.

			Pseudo-First order			Pseudo-Second order		
	C_e (g/L)	$q_{e,exp}$ (mg/g)	$q_{e,cal}$ (mg/g)	$K_{ads,1}$ (min^{-1})	R^2	$q_{e,cal}$ (mg/g)	$K_{ads,2}$ (min^{-1})	R^2
Pods	0.5	38.876	1.384	-6.66667	0.104	38.462	0.027	0.999
	1	19.526	1.313	-0.0001	0.163	18.182	0.059	0.998
	2	9.782	0.204	-0.000075	0.563	9.804	0.101	0.999
	3	6.643	0.145	9.16667	0.206	7.353	0.125	0.999
Kernels	0.5	37.685	4.7350	-0.000075	0.263	38.462	0.024	0.997
	1	18.479	0.32628	-0.000258	0.034	22.728	0.0340	0.996
	2	8.970	5.65195	-0.014608	0.136	11.364	0.044	0.996
	3	6.119958	0.746022	-3.33333	0.069	5.747126	0.179	0.997

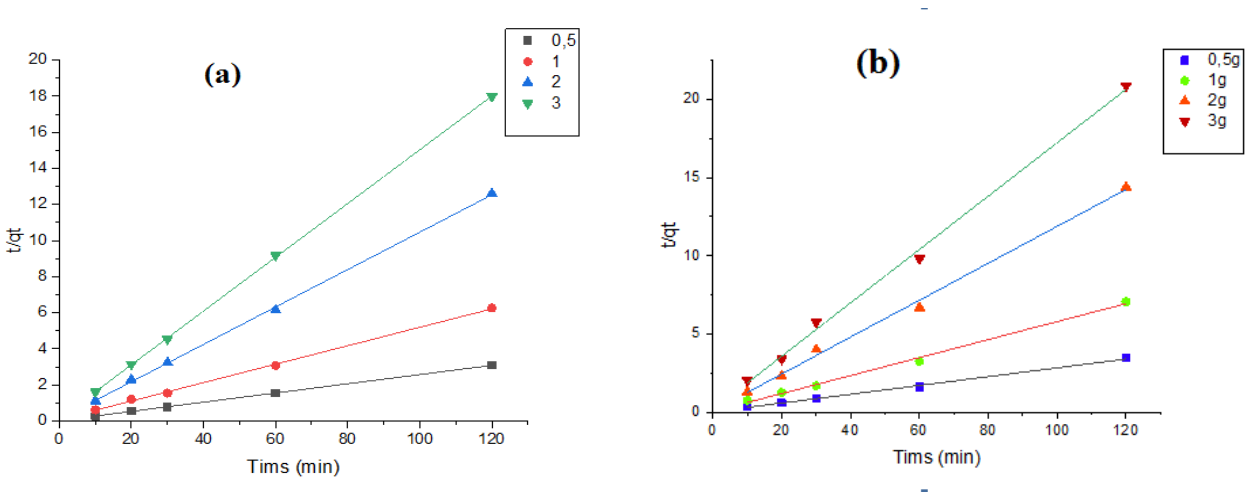

Fig. 12: Application of the pseudo-second order model for MB adsorption onto pods (a) and kernels (b)

The plots of linear equation of the pseudo-second-order model were found linear with good correlation coefficients (R^2) for the pseudo-second-order kinetic model. Further, the calculated q_e values using the pseudo-second order kinetic model were also found in accordance with the experimental uptake values $q_{e,exp}$, contrary to the values determined by the pseudo-first kinetic model which are smaller than the

experimental data, which means that the pseudo-second-order model describes correctly the biosorption kinetics. Similar phenomena processes have been observed in the adsorption of methylene blue and methyl orange by the mixture of palm waste (Azoulay et al., 2020) and adsorption of Rhodamine B and Alizarin Red S dye on calcined waste of eggshells (Slimani et al., 2021).

3.4. Adsorption isotherms study

In order to optimize the adsorption process, it is essential to describe the quantity adsorbed by a given amount of adsorbent. The experimental data were fitted into equilibrium adsorption isotherm models of Freundlich, Langmuir and Temkin. The equations and linearized form of these isotherm models are given in Table 2.

Table 2. Isotherm models tested in this study

Isotherm	Non linear form	Linear form
Langmuir	$\frac{q_e}{q_m} = \frac{K_L C_e}{1 + K_L C_e}$	$\frac{C_e}{q_e} = \frac{1}{q_m K_L} + \frac{C_e}{q_m}$
Freundlich	$q_e = K_F C_e^{n}$	$Log(q_e) = log(K_F) + n\ log\ (C_e)$
Temkin	$\frac{q_e}{q_m} = \frac{RT}{\Delta Q} \ln(K_T C_e)$	$q_e = B_T \ln K_T + B_T \ln C_e$ (with $B_T = \frac{q_m RT}{\Delta Q}$)

The application of the Langmuir model to the present experimental data gave a poor fit, however, so that it is clearly not appropriate for the Methylene Blue on the pods and the kernels seeds of *Moringa oleifera* adsorbent. While the application of the Freundlich and Temkin isotherm models show a good regression coefficient compared to Langmuir model before cited (**Table 3**). The R^2 values for kernels and pods indicate good agreement between the experimental values and the Freundlich isotherm parameters for MB adsorption onto both substrates.

Table 3. Isotherm parameters for Methylene Blue adsorption onto the pods and the Kernels of *Moringa oleifera*

	Isotherm model	Parameters		
Pods	**Langmuir**	q_m= 169.49 mg/g	K_L = 0.28 mg/g	R^2 = 0.77
	Freundlich	K_F = 30.63 $mg^{1-n} L^n/g$	n = 0.53	R^2 = 0.96
	Temkin	K_T = 1.78 L/mg	B_T = 33.86	R^2 = 0.99
Kernels	**Langmuir**	q_m=158.73 mg/g	K_L = 0.07 mg/g	R^2 = 0.82
	Freundlich	K_F = 3.28 $mg^{1-n} L^n/g$	n = 0.63	R^2 = 0.92
	Temkin	K_T = 1.92L/mg	B_T = 29.89	R^2 = 0.98

Based on the fundamentals of the Freundlich theory, it can be concluded that the biosorption process most likely occurs in more than one layer (heterogenous surfaces). This means a linear adsorption, leading to identical adsorption energies for all sites (Novaisetal., 2018). The results corroborate with the study of Soliman et al., in 2019 in removal of Congo red and Dispersed red 60 dyes using *Moringa oleifera* seeds waste as adsorbent. Additionally, the Temkin model with high correlation coefficient

confirm that the adsorption of methylene blue onto the pods and the kernels seeds of Moringa oleifera follows a chemisorption process. Similarly, Elmorsi et al. used the Temkin isotherm model in their investigation of the adsorption of methylene blue onto miswak leaves (Elmorsi. M., 2011).

3.5. Thermodynamic studies

In liquid phase adsorption, adsorption occurs as solvent species are removed from the adsorption sites. Displacement enthalpies are key factors in this process, since they balance different weak interactions between the adsorbent, adsorbate, and solvent. The free energy variation (ΔG°) of the adsorption reaction is expressed by the following equation (Araujo *et al.,* 2018):

$$\Delta G° = -RT.\ln K_d \qquad \textbf{(Eq. 3)}$$

The values of ΔH° and ΔS° can be determined from the graph of $\ln K_d$ versus 1/T and T is the absolute temperature in Kelvin. The values of ΔH° and ΔS° can be determined from the slope ($\Delta H°$/R) and intercept ($\Delta S°$/R) of the graph (**Figure 13**) of $\ln K_d$ versus 1/T (Araujo *et al.,* 2018) using the equation of Van't Hoff as expressed below:

$$lnK_d = \frac{\Delta S°}{R} - \frac{\Delta H°}{RT} \qquad \textbf{(Eq. 4)}$$

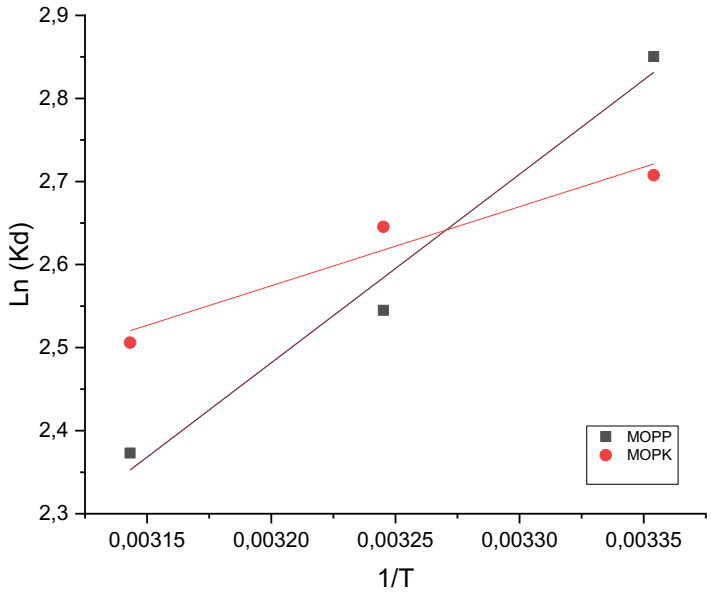

Fig. 13. Plots of lnKd vs. 1/T for the biosorption studies of MB onto the pods and the kernels powder of *Moringa oleifera*.

The calculated values of ΔH°, ΔS° and ΔG° obtained from the experimental data at different temperatures for the biosorption of Methylene Blue adsorption onto the pods powder and the kernels powder of *Moringa oleifera* are listed in **Table 4**. The negative values of ΔH° of pods and kernels are respectively (-7.892 KJ.mol^{-1}), (-18.873 KJ.mol^{-1}) confirmed the exothermic interaction between the organique pollutants Methylen Bleu biosorbates and the pods and the kernels of *Moringa oleifera* waste biosorbents (Reck et al., 2018). So the nature of the adsorption process is exothermic. Moreover, the negative values of ΔS° (-3.766 J. mol-1.K^{-1}) (-39.783 J.mol-1.K^{-1}) revealed a decrease in the level of dispersion of the process at the solid/solution interface during the adsorption of MB on pods and

kernels. However, the negative and increase values of the ΔG° at the studied temperature range in **Table 4** indicated that the adsorption of methylene bleu on adsorbent was thermodynamically feasible and spontaneous which confirms that the nature of adsorption process is physical (Rahmani *et al.,* 2021).

Table 4. Thermodynamic parameters for MB adsorption on pods and kernels of Moringa oleifera.

	T	ΔG (KJ/mol)	ΔH (KJ/mol)	ΔS (J/mol*K)	R^2
Pods	298	-6.71	-7.92	-3.77	0.945
	308	-6.78			
	323	-6.63			
Kernels	298	-7.07	-18.87	-39.78	0.98
	308	-6.52			
	323	-6.28			

Conclusion

In this work. the waste products of Moringa oleifera were used for the removal of MB from the aqueous solution. The results obtained relating to the kinetics. isotherms and thermodynamics of adsorption were exploited to clarify the mode of dye fixation on the adsorbent. It is found that equilibrium is reached from 30 min and adsorption capacity of MOPP and MOPK waste increases with the increase of the initial MB concentration. Moreover. the adsorption process follows the pseudo-second order model with R^2 close to 1 for both wastes (MOPP and MOPK). According to the intra-particle diffusion results the adsorption process occurs in two stages for both wastes. of which the first stage was fast and then slows down in the second stage. In addition. the Freundlich isotherm is the best isotherm which describes the adsorption phenomenon for the two wastes studied.

Conflict of interest

The authors declare that they have no conflicts of interest in relation to this article.

Disclosure statement: *Conflict of Interest:* The authors declare that there are no conflicts of interest.
Compliance with Ethical Standards: This article does not contain any studies involving human or animal subjects.

References

Alsharaa A., Basheer C., Adio S.O., Alhooshani K., Lee H, K. (2016) Removal of haloethers. trihalomethanes and haloketones from water using Moringa oleifera seeds. *International Journal of Environmental Science and Technology,* 13, 2609-2618.

Alves V.N., Mosquito R., Coelho N. M. M., Blanching J. N., Roux K.C.D., Martindale E., Crease E. (2010) Determination of cadmium in alcohol fuel using Moringa oleifera seeds as a bio sorbent in an on-line system coupled to FAAS. *Talanta,* 80, 1133-113.

Araújo C. S. T., Melo, E. I., Alves, V. N., & Coelho, N. M. M. (2010) *Moringa oleifera Lam.* seeds as a natural solid adsorbent for removal of AgI in aqueous solutions. *Journal of the Brazilian Chemical Society,* 21(9), 1727-173.

Araujo L. A., Charleston, O. B., Luıs, F. C., Silva, M. F., Nishi, R. G. L., Gomes, R. B. (2018) Moringa oleifera biomass residue for the removal of pharmaceuticals from water. *Journal of Environmental Chemical Engineering,* 6(6), 7192-7199.

Arrakhiz F. Z., Achaby, M. E., Malha, M., Bensalah, M., Fassi-Fehri, O., Bouhfid, R., Benmoussa, K., Qaiss, A. (2013) Mechanical and thermal properties of polymer composites reinforced with natural fibers: Doum / low density polyethylene. *Materials and Design,* 43, 200-205.

Aysan H., Edebali, S., Ozdemir, C., Karakaya, M. C., Karakaya, N. (2016) Use of chabazite. a naturally abundant zeolite. for the investigation of the adsorption kinetics and mechanism of methylene blue dye. *Microporous Mesoporous Mater,* 235, 78-86.

Azoulay K., Bencheikh, I., Moufti .A., Dahchour, A., Mabrouki, J., El Hajjaji, S. E. (2020) Comparative study between static and dynamic adsorption efficiency of dyes by the mixture of palm waste using the central composite design. *Chemical Data Collections,* 27, 100385.

Baptista A. T. A., Silva, M. O., Gomes, R. G., Bergamasco, R., Vieira, M. F., Vieira, A. M. S. (2017) Protein fractionation of seeds of Moringa oleifera lam and its application in superficial water treatment. *Sep. Purif. Technol*., 180, 114-124.

Bencheikh I., Azoulay, K., Mabrouki, J., Hajjaji, E. S., Moufti, A., Labjar, N. (2021) The use and the performance of chemically treated artichoke leaves for textile industrial effluents treatment. *Chemical Data Collections,* 31, 100597.

Bouknana D., Hammouti B., Salghi R., Jodeh S., Zarrouk A., Warad I., Aouniti A., Sbaa M. (2014) Physicochemical characterization of olive oil mill wastewaters in the eastern region of Morocco, *J. Mater. Environ. Sci.* 5 (4), 1039-1058

Çelekli A., Al-Nuaimi, A. I., Bozkurt, H. (2019) Adsorption kinetic and isotherms of Reactive Red 120 on Moringa oleifera seed as an eco-friendly process. *Journal of Molecular Structure*, 1195, 168-178.

Camacho F. P., Sousa, V. S., Bergamasco, R., Teixeira, R. M., (2017) The use of Moringa oleifera as a natural coagulant in surface water treatment. *Chem. Eng. J.,* 313, 226-237.

Cardoso S. L., Costa, C. S. D., Nishikawa, E., Silva, M. G. C., Vieira, M. G. A. (2017) Biosorption of toxic metals using the alginate extraction residue from the brown algae Sargassum filipendula as a natural ion-exchanger. *J. Clean. Prod.,* 165, 491-499.

Djelloul C., Hasseine, A., Hamdaoui, O. (2017) Adsorption of cationic dye from aqueous solution by milk thistle seeds: isotherm. kinetic and thermodynamic studies. Desalination and Water Treatment, 78, 313-320.

El Hammari L., Latifi S., Saoiabi S., Azzaoui K., Hammouti B., Chetouani A., Sabbahi R. (2022) Toxic heavy metals removal from river water using a porous phospho-calcic hydroxyapatite, *Mor. J. Chem.* 10, 62-72, https://doi.org/10.48317/IMIST.PRSM/morjchem-v10i1.31752

Elmorsi T. M. (2011) Equilibrium isotherms and kinetic studies of removal of methylene blue dye by adsorption onto miswak leaves as a natural adsorbent. *Journal of Environmental Protection*, 2(6), 817-827.

Ezeamaku U. L., Chike-Onyegbula, C. O., Iheaturu, N. C., Onwuka E. O., Ezike C. C., Onuchukwu, S.T. (2018) Treatment of lead contaminated wastewater using aluminium sulphate and *Moringa oleifera* as coagulants. *Nigerian Journal of Polymer Science And Technology,* 13, 82 -92.

Filho A. C. D., Mazzocato, A. C., Dotto, G. L., Thue. P. S., Pavan. F. A. (2017) *Eragrostisplana Nees* as a novel eco-friendly adsorbent for removal of crystal violet from aqueous solutions. *Environmental Science and Pollution Research,* 24(24) 19909-19919.

Ghasemi J., Asadpour, S. (2007) Thermodynamics study of the adsorption process of methylene blue on activated carbon at different ionic strengths. *J. Chem. Thermodyn.,* 39, 967-971.

Gupta V. K., Carrott, P. J. M., Singh, R., Chaudhary, M., and Kushwaha, S. (2016) Cellulose: A review as natural. modified and activated carbon adsorbent. *J. Bioresour. Technol.,* 216, 1066-1076.

Hu Z., Chen, H., Ji, F., Yuan, S. (2010) Removal of Congo Red from aqueous solution by cattail root. *J. Hazard. Mater.,* 173(1), 292-297.

Kali A., Dehmani Y., Loulidi I., Amar A., Jabri M., El-kord A., Boukhlifi F. (2022) Study of the adsorption properties of an almond shell in the elimination of methylene blue in an aquatic, *Mor. J. Chem.* 10, 509-522, https://doi.org/10.48317/IMIST.PRSM/morjchem-v10i3.33140

Karouia S., Arfi, R. B., Mougin, K., Ghorbal, A., Assadi, A. A., Amrane, A. (2020) Synthesis of novel biocomposite powder for simultaneous removal of hazardous ciprofloxacin and methylene blue: Central composite design. kinetic and isotherm studies using Brouers-Sotolongo family models. *Journal of Hazardous Materials,* 387, 121675.

Maina I. W., Obuseng, V., Nareetsile, F. (2016) Use of moringa oleifera (moringa) seed pods and sclerocaryabirrea (Morula) nut shells for removal of heavy metals from wastewater and borehole water. *J. Chem.,* 2016, 9312952, https://doi.org/10.1155/2016/9312952

Mansour H. B., Boughzala O., Dridi, D., Barillier D., Chekir-Ghedira L., Mosrati R. (2011) Les colorants textiles sources de contamination de l'eau : Criblage de la toxicité et des méthodes de traitement. *Revue Des Sciences de l'Eau,* 24, 209-239. https://doi.org/10.7202/1006453ar

Novais R. M., Ascensão G., Tobaldi D. M., Seabra M. P., Labrincha J. A. (2018) Biomass fly ash geopolymer monoliths for effective methylene blue removal from wastewaters. *Journal of Cleaner Production*, 171, 783-794.

Oba I. A., Adekola F. A. (2018) Kinetic and thermodynamic adsorption study of formic and acetic acids from aqueous solution by activated carbon derived from moringa oleifera pods, *Mor. J. Chem.* 6 (3), 492-503

Olsson A. M., Salmén L., (2004) The association of water with cellulose and hemicellulose in the paper examined by FTIR spectroscopy. *Carbohydrate Research,* 339 (4), 813-818.

Paiva M. C., Ammar I., Campos A. R., Cheikh R. B., Cunha A., Alfa M. (2007) Fibers: Mechanical, Morphological and Interfacial Characterization. *Composites Science and Technology*, 67 (6) 1132-1138.

Rahmani M., Mabrouki J., Regraguy B., El Hajjaji S. (2021) Adsorption of (methylene blue) onto natural oil shale: kinetics of adsorption. isotherm and thermodynamic studies. *International Journal of Environmental Analytical Chemistry*, 1(15), 1957466.

Ravikumar K., Udayakumar J. (2020) *Moringa oleifera* biopolymer coagulation and bentonite clay adsorption for hazardous heavy metal removal from aqueous systems. *Geosystems Engineering,* 23, 265-275. https://doi.org/10.1080/12269328.2020.1778544

Reck I. M., Paixao R. M., Bergamasco R., Vieira M. F., Salcedo Vieira, A. M. (2018) Removal of tartrazine from aqueous solutions using adsorbents basedon activated carbon and Moringa oleifera seeds. *Journal of Cleaner Production,* 171, 85-97.

Sgriccia N., Hawley M. C., Misra M. (2008) Characterization of Natural Fiber Surfaces and Natural Fiber Composites. *Composites Part A: Applied Science and Manufacturing*, 39, 1632-1637.

Shirani Z., Santhosh C., Iqbal J., Bhatnagar A. (2018) Waste Moringa oleifera seed pods as green sorbent for efficient removal of toxic aquatic pollutants. *Journal of Environmental Management,* 227, 95-106.

Shooto N. D., Thabede P. M., Bhila B., Moloto H., Naidoo E. B. (2020) Lead ions and methylene blue dye removal from aqueous solution by mucuna beans (velvet beans) adsorbents. *Journal of Environmental Chemical Engineering*. 8(2), 103557.

Singh H., Chauhan G., Jain, A. K., Sharma S. K. (2017) Adsorptive potential of agricultural wastes for removal of dyes from aqueous solutions. *J. Environ. Chem. Eng.,* 5, 122-135.

Slimani R., El Ouahabi I., Benkaddour S., Hiyane H., Essoufy M., Achour Y., El Antri S., Lazar S., El Haddad. M. (2021) Removal efficiency of textile dyes from aqueous solutions using calcined waste of eggshells as eco-friendly adsorbent: Equilibrium. Kinetic. Isotherm and thermodynamic studies. *Chemical and Biochemical Engineering Quarterly*, 35(1), 43-56.

Soliman N. K., Moustafa A. F., Aboud A. A., Saad A. K. (2019) Effective utilization of *Moringa* seeds waste as a new green environmental adsorbent for removal of industrial toxic dyes. *Journal of Materials Research and Technology,* 8(2), 1798-1808.

Utrilla J. R., Toledo I. B., Garcia M. A. F., Castilla C. M. (2001) Activated carbon surface modifications by adsorption of bacteria and their effect on aqueous lead adsorption. *J. Chem. Technol. Biot.,* 76, 1209-1215. https://doi.org/10.1002/jctb.506

(2023) ; https://revues.imist.ma/index.php/morjchem/index